

# THE GALAXY STRUCTURE-REDSHIFT RELATIONSHIP

Christopher J. Conselice<sup>1</sup>

<sup>1</sup>*California Institute of Technology, Pasadena, CA USA*

## Abstract

There exists a gradual, but persistent, evolutionary effect in the galaxy population such that galaxy structure and morphology change with redshift. This galaxy structure-redshift relationship is such that an increasingly large fraction of all bright and massive galaxies at redshifts  $2 < z < 3$  are morphologically peculiar at wavelengths from rest-frame ultraviolet to rest-frame optical. There are however examples of morphologically selected spirals and ellipticals at all redshifts up to  $z = 3$ . At lower redshift, the bright galaxy population smoothly transforms into normal ellipticals and spirals. The rate of this transformation strongly depends on redshift, with the swiftest evolution occurring between  $1 < z < 2$ . This review characterizes the galaxy structure-redshift relationship, discusses its various physical causes, and how these are revealing the mechanisms responsible for galaxy formation.

**Keywords:** Galaxy Formation/Evolution, Galaxy Structure, Galaxy Morphology

## 1. Introduction

The structures and morphologies of galaxies change with time. Determining the history and cause of this galaxy structure-redshift relationship, including the origin of modern galaxy morphologies (i.e., ellipticals, disks) is perhaps the missing, and until now overlooked, link in understanding galaxy formation. While we currently have a good understanding of global galaxy formation and evolution, such as the star formation and mass assembly history (e.g., Madau et al. 1996; Dickinson et al. 2003), we are only beginning to understand *how* galaxy formation occurs as opposed to simply when. During the last few years it has become clear with the advent of wide-field imaging surveys from the ground, and from space using the Hubble Space Telescope, that galaxy structure evolves (e.g., Driver et al. 1995; Glazebrook et al. 1995; Abraham et al. 1996; Brichmann & Ellis 2000; Conselice et al. 2004b). There is a clear galaxy structure (or morphology)-redshift relationship such that galaxies in the more distant universe are peculiar while those in the local universe are more regular

or normal<sup>1</sup> (van den Bergh et al. 2001). Determining the physics behind the morphology-redshift relationship is critical for any ultimate understanding of galaxies and the physical causes of galaxy structure and its evolution.

The morphology-redshift relationship can furthermore potentially be used as a key test of galaxy formation models. Theories of galaxy formation can be divided into two main ideas - the monolithic collapse of material early in the universe to form stars and galaxies within a very short time (e.g., Larson 1975; Tinsley & Gunn 1976) and the hierarchical formation scenario (e.g., White & Rees 1978; Blumenthal et al. 1984; White & Frenk 1992; Cole et al. 2000). Observationally, we know that galaxies do not appear to form rapidly in the early universe, but have an extended star formation history that does not decline significantly until the universe is about half its current age. Likewise, about half of all stellar mass in the universe formed between  $z \approx 1$  (8 Gyrs ago) and today (Dickinson et al. 2003). The fact that star formation occurs over time, and not quickly at very high redshift, largely rules out rapid collapses as the primary method for forming all galaxies. High redshift galaxies also tend to be small with likely small stellar masses (Papovich et al. 2001; Ferguson et al. 2004). Therefore a large fraction of all galaxies must have formed gradually throughout time. Understanding this process, that is what is causing mass to build up in galaxies, requires studying their internal properties.

There are several ways to measure the physical processes responsible for forming galaxies which can potentially explain the observed morphology-redshift relationship (x3). One method, and by far the most common, is to study global galaxy properties, such as the evolution of stellar mass and star formation, and to compare these with predictive models (e.g., Somerville et al. 2001). Other methods, which are now just being explored, involve probing the internal features of high- $z$  galaxies either through spectroscopy or high resolution imaging. While integral field spectroscopy for high- $z$  galaxies is still in its infancy, understanding the internal structural features of high redshift galaxies is now in a golden age, utilizing new techniques (e.g., Conselice et al. 2000a; Peng et al. 2002) with high resolution Hubble Space Telescope imaging (e.g., Giavalisco et al. 2004; Rix et al. 2004).

The idea that the structures of galaxies hold clues towards understanding their current and past formation histories is a new, and perhaps still controversial, idea. There is however increasing amounts of evidence that suggests galaxy structure reveals fundamental past and present properties of galaxies (see Conselice 2003 and references within and x2). Utilizing these tools, we

---

<sup>1</sup>Throughout this review, I refer to 'regular' or 'normal' galaxies to denote systems that are on the present day Hubble sequence; namely ellipticals and spirals. Peculiar galaxies and/or mergers are not normal galaxies according to this criteria. This differs from the usual meaning of normal which refers to galaxies without the presence of an active galactic nuclei (AGN).

can begin to determine the origin of the galaxy morphology-redshift relationship. Understanding this relationship will in turn help us determine physical formation mechanisms, and the history of galaxy assembly. Furthermore, it is now possible to compare observations of the galaxy morphology-redshift relationship with theoretical models based on cosmological and dark matter ideas, connecting the universe as a whole to its constituent galaxies. I argue in this review that the galaxy morphology-redshift relationship is a pillar for understanding galaxy formation. It may also hold clues for understanding the relationship between the baryonic content of galaxies and their dark matter halos, the evolution of galaxies and their black holes, and the relationship between cosmological parameters and the evolution of galaxy structure. In summary, I will address in detail the following issues:

- (i) What is the galaxy structure-redshift relationship and how does it evolve?
- (ii) What are the physical causes for the formation and evolution of the galaxy structure-redshift relationship?
- (iii) What does the evolution of the galaxy-structure redshift relationship tell us about galaxy formation?

I do not address some morphological evolution problems, such as the formation and evolution of bars, rings or other internal structures, as these are dealt with in other contributions (e.g., Jogee, Sheth). Throughout I will assume a cosmology with  $H_0 = 70 \text{ km s}^{-1} \text{ Mpc}^{-1}$  and relative densities of  $\Omega_b = 0.04$  and  $\Omega_m = 0.3$ .

## 2. The Physical Basis of Galaxy Structure

Before describing the galaxy morphology-redshift relationship, and what it implies for understanding galaxy formation, I will review our current understanding of how galaxy structure correlates with physical properties of galaxies. It has been known for decades that, broadly speaking, galaxy morphology correlates with galaxy properties such as luminosities, sizes, gas content, colors, environment, masses, and mass to light ratios (e.g., Roberts & Haynes 1994). Generally, early-type galaxies (ellipticals) are larger, more massive, contain older stellar populations, and are found in denser areas than spirals. Later type galaxies, such as spirals, are bluer, contain younger stellar populations, more gas, and are less massive overall than the ellipticals. The detailed correlation between these physical properties and Hubble/de Vaucouleur classifications is however not strong. While in the mean properties change with Hubble type, there is significant overlap in any given property across the Hubble sequence<sup>2</sup>.

---

<sup>2</sup>Room prohibits a detailed discussion of all the problems with Hubble classifications. The fact that physical properties only correlate in the mean for a given Hubble type is only one of many issues. For a detailed

*Table 1.* The co-moving densities of bright ( $M_B < -20$ ) galaxies as a function of morphological type in units of  $\log(\text{Gpc}^{-3})^a$

Redshift	Ellipticals	Spirals	Peculiars
0.0	6.41 0.01	6.98 0.01	5.34 0.03
0.5	6.3 0.2	6.6 0.1	5.7 0.2
0.8	6.3 0.2	6.2 0.2	5.4 0.3
1.0	6.4 0.2	6.5 0.2	6.1 0.2
1.2	6.2 0.2	6.1 0.2	5.7 0.3
1.3	6.0 0.2	5.9 0.2	6.3 0.2
1.5	5.7 0.2	...	5.4 0.3
1.6	...	5.4 0.3	5.7 0.3
1.7	5.4 0.3	5.7 0.2	6.1 0.2
1.9	5.7 0.2	5.4 0.4	5.7 0.3
2.0	5.9 0.2	6.1 0.2	6.4 0.1

<sup>a</sup>Galaxies at  $z = 0$  are taken from the “Third Reference Catalogue of Bright Galaxies” (de Vaucouleurs et al. 1991). The other galaxy densities at  $z > 0$  are an average between the densities found for each type in the Hubble Deep Fields North and South.

Some quantitative measurements of galaxy structure, on the other hand, correlate strongly with physical properties, including: the current star formation rate, the stellar mass, galaxy radius, central black hole mass, and merging properties. It is impossible to describe all but a few of these correlations here. The first of these discovered is that the light concentration of an evolved stellar population correlates with its luminosity, stellar mass, and scale (e.g., Caon, Capaccioli & D’Onofrio 1993; Graham et al. 1996; Bershadsky et al. 2000; Conselice 2003). This was first noticed by the failure of the de Vaucouleurs  $r^{1=4}$  surface brightness profile to fit the surface brightness distributions of elliptical galaxies brighter than or fainter than  $M_B = -20$  (e.g., Schombert 1986). It was realized later that the shape of the surface brightness profile for early types correlates strongly with its absolute blue magnitude (Binggeli & Cameron 1991; Caon et al. 1993). It was later shown that the general Sersic profile, with its concentration parameter  $n$ , gives a much better fit than the de Vaucouleur’s profile for all early types (Graham et al. 1996). The central light concentration, as measured through the Sersic  $n$  index, or a non-parametric concentration index ( $C$ ) (Bershadsky et al. 2000), also correlates with the mass of central black holes (Graham et al. 2001).

While the concentration of a galaxy’s light profile correlates with its stellar mass, absolute magnitude, and size, in a sense revealing the past formation

---

discussion of this see Appendix A from Conselice (2003). It is still useful to separate in the broadest sense, ellipticals from spirals, as I do here, as these are fundamentally different galaxy types.

history of a galaxy, there are many indicators in the structures of galaxies for ongoing galaxy formation. For example, recently it has been shown that the clumpiness of a galaxy's light distribution correlates with the amount and the location of star formation (e.g., Takamiya 1999; Conselice 2003). The clumpiness is measured by quantifying the fraction of a galaxy's light in the rest-frame B-band in high spatial frequency structures. The ratio between the amount of light in these high spatial frequency structures and the total light gives a measure of the clumpiness, or star formation. This trend can be demonstrated by the strong correlation between the clumpiness index  $S$  (Conselice 2003) and  $H\alpha$  equivalent widths and colors of star forming galaxies. There is also a strong relationship between the dynamical state of a galaxy and the presence of a merger. Generally, merging galaxies are asymmetric, while non-mergers are not (Conselice et al. 2000a,b; Conselice 2003). This has been shown in numerous ways, including empirical methods (Conselice 2003) and the correlation of internal HI dynamics and asymmetries of stellar distributions (Conselice et al. 2000b).

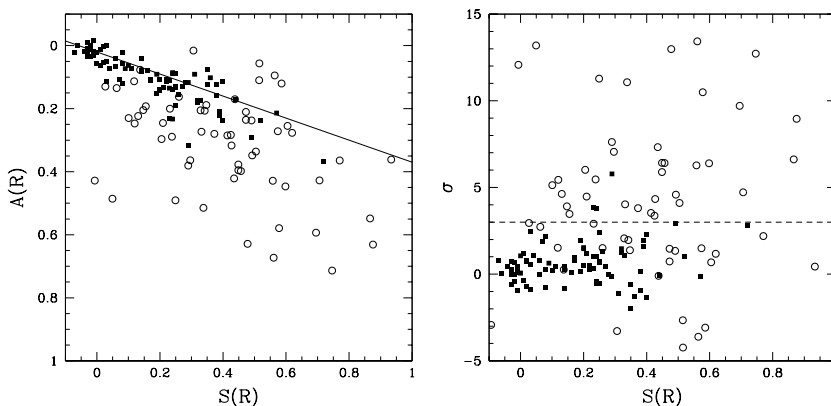


*Figure 1.* The relationship between the asymmetry index ( $A$ ) and the clumpiness index ( $S$ ). Higher  $A$  and  $S$  values indicate galaxies that are more asymmetric and have a higher fraction of clumpy light, respectively. For normal galaxies (black squares, left panel) there is a strong correlation between  $A$  and  $S$  such that  $A = (0.35 \pm 0.03) S + (0.02 \pm 0.01)$ . The galaxies which deviate from this relationship are the ongoing major mergers, shown in the left panel as open circles. The right panel shows the deviation from the  $A - S$  relationship in units of the scatter of the asymmetry values of the normal galaxies ( $\sigma$ ). Generally, only the mergers deviate from this relationship by more than  $3\sigma$ . For a physical reasoning behind these correlations see the text and Conselice (2003).

As shown in Conselice et al. (2000a) asymmetric light distributions can also be caused by star formation. However, by decomposing light and kinematic structures in galaxies, it is possible to show that primary asymmetries

are not the result of star formation, which forms in clumps (e.g., Elmegreen 2002), but from large scale lopsidedness on the order of the size of the galaxy itself (Andersen et al. 2001). Likewise, there is a strong correlation between the asymmetry parameter and the clumpiness parameter for normal star forming galaxies (Conselice 2003; Figure 1). Galaxies with high clumpiness values ( $S$ ), which correlates with high amounts of star formation, have correspondingly higher asymmetry values. However, this correlation breaks down for systems involved in major mergers, such as nearby ultraluminous infrared galaxies (Figure 1). The nature of this deviation is such that a galaxy undergoing a merger has too high an asymmetry for its clumpiness, demonstrating that large asymmetries are produced in large scale features and not in clumpy, star formation like regions (Conselice 2003; Mobasher et al. 2004; Figure 1)<sup>3</sup>.

### 3. The Galaxy Morphology-Redshift Relationship

#### 3.1 Summary

The summary figure for understanding the galaxy structure-redshift relationship is Figure 2. This relationship can be summarized simply as: *At higher redshifts (early times) the fraction of bright galaxies that are peculiar in structure and morphology increases gradually at the expense of both spirals and ellipticals.*

The final state of galaxy evolution surrounds us, and the modern universe is dominated by galaxies that can be classified on the Hubble sequence. A large fraction of all modern massive and bright galaxies are either ellipticals or spirals; only roughly 1-2% of all bright galaxies with  $M_B < -20$  can be classified as peculiars (e.g., Marzke et al. 1998) (see Table 1). This changes gradually with redshift up to  $z \approx 1$  and then more rapidly between  $1 < z < 2$ ; at  $z \approx 1$  most galaxies have relaxed morphologies while at  $z \approx 2$  most galaxies are peculiar (Conselice et al. 2004b; Table 1).

#### 3.2 Galaxy Structures at Low Redshift $z < 1$

At redshifts  $z < 1$  most of the bright ( $M_B < -20$ ) and massive galaxies ( $M > 10^{10}$ ) are normal galaxies, that is ellipticals and spirals (Table 1; Figure 2). This relative fraction remains largely similar out to  $z \approx 1$ , with some important exceptions. In general, the co-moving density of elliptical and disk

---

<sup>3</sup>The concentration index ( $C$ ), asymmetry index ( $A$ ), and clumpiness index ( $S$ ) form the CAS morphology system described in detail in Conselice (2003). With these three parameters the major classes of nearby galaxies can be distinguished. Although this idea is not explicitly described in this review, it is used in papers described here, such as Conselice et al. (2004b) and Mobasher et al. (2004) to determine galaxy types.

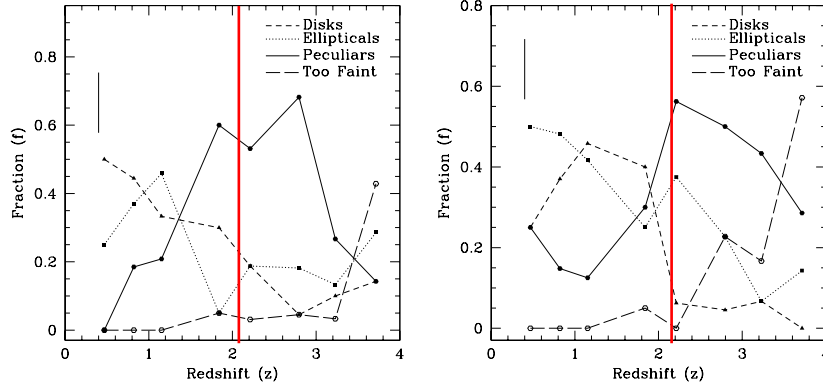


**Figure 2. The galaxy structure-redshift relationship.** This figure shows the evolution in relative fractions of different galaxy types as a function of redshift for classifications in the  $I_{814}$  (left panel) and  $H_{160}$  (right panel) band images of the HDF-N. The short vertical solid line on each plots gives the average error for these fractions. The long vertical line is the redshift limit for detecting spirals and ellipticals with  $M_B < -20$ . Types plotted are: disks (short dashed), ellipticals (dotted), peculiars (solid) and galaxies which are too faint for a classification (long dashed).

galaxies remains constant, to within a factor of 2, out to  $z \approx 1$  with a slight decline (Figure 3; Brinchmann & Ellis 2000; Conselice et al. 2004b).

There is a more pronounced change in other features of normal galaxies from  $z \approx 1$  to  $z \approx 0$ . These properties include co-moving B-band luminosity densities ( $L_B$ ), and stellar mass densities ( $\rho$ ). While the number density evolution of Hubble types is the physical manifestation of the galaxy structure-redshift relationship, the evolution of other properties can reveal important clues for how this relationship is put into place, and why it might be evolving. The rest-frame B-band luminosity density evolution for galaxies of known morphology is shown in Figure 3. There is a clear decline with cosmic time in luminosity densities at  $z < 1$  for all galaxies, including ellipticals and spirals. This peak in the B-band luminosity density at  $z \approx 1$  is produced in normal galaxies, and must be due to recent star formation, as the stellar mass density for normal galaxies grows with time (Figure 3). The stellar mass density for ellipticals is half of its modern value at  $z \approx 1$  in the Hubble Deep Field North (HDF-N). There is perhaps an over density of ellipticals at  $z \approx 1$  in the HDF-N, and cosmic variance is an issue. Although a lower density of early types would only enhance the evolution in stellar mass for these systems. This effect is also seen in studies considering galaxies on the ‘red sequence’, defined by the tight correlation between magnitude and color for early types. The stellar mass in red sequence galaxies increases by a factor of two from

$z = 1$  to  $z = 0$  (Bell et al. 2004), exactly the increase found when considering morphologically selected early types. Because of the large amount of co-moving luminosity in normal galaxies at  $z \approx 1$ , star formation must be occurring in early type galaxies during this time (see also Stanford et al. 2004). Luminosity and stellar mass functions suggest that this evolution is occurring in lower mass and lower luminosity systems (Conselice et al. 2004b), while the higher mass systems are perhaps largely formed by  $z \approx 1$ , or even earlier (e.g., Glazebrook et al. 2004).

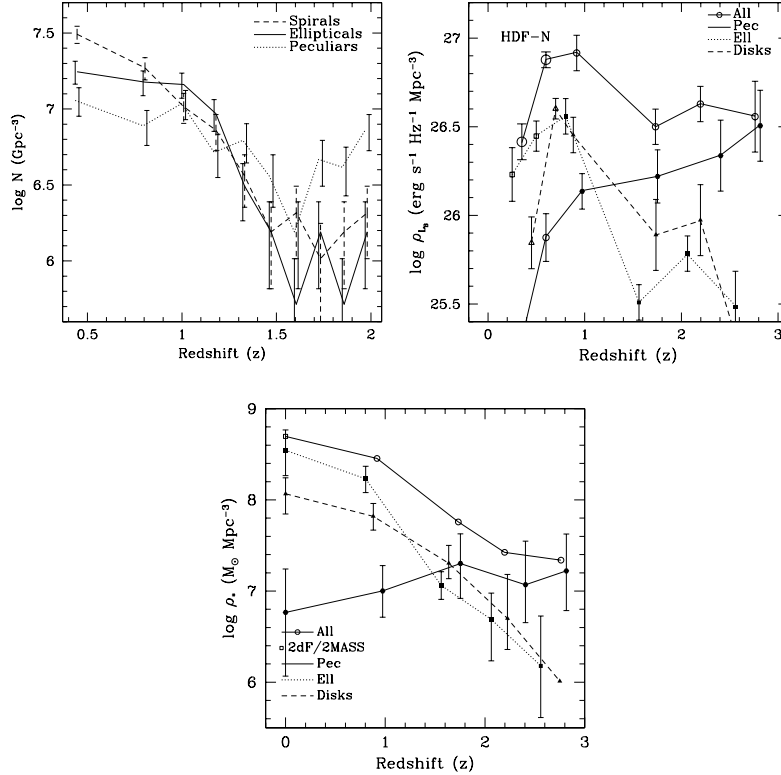


*Figure 3.* The relative co-moving number ( $N$ ), rest-frame B-band luminosity ( $\rho_L$ ), and stellar mass density ( $\rho_*$ ) of galaxies as a function of redshift from deep NICMOS imaging of the Hubble Deep Field North (Conselice et al. 2004b). Points at redshifts  $z < 0.5$  are taken from Brinchmann & Ellis (2000), Fukugita et al. (1998) and the 2dF/2MASS surveys (Cole et al. 2001).

### 3.3 Galaxy Structures at Medium Redshift $1 < z < 2$

Morphological counts of galaxies from early Hubble Space Telescope imaging found a large increase in the number of peculiar/irregular galaxies at fainter magnitudes (e.g., Driver et al. 1995; Glazebrook et al. 1995). It was however unknown during these early Hubble observations what the redshifts, and therefore the characteristics, of these peculiar galaxies were. When redshifts for these faint galaxies became available, it was argued that Hubble types appeared in abundance by  $z \approx 1$ , and evolve only slightly down to lower redshifts (van den Bergh et al. 2001; Kajisawa & Yamada 2001).

Ultimately what is desired is a determination of Hubble types as a function of redshift for galaxies of different luminosities and stellar masses. This was performed for bright galaxies in the Hubble Deep Field North and South by Conselice et al. (2004b). The results of this are shown in Figure 3 for galaxies brighter than  $I = 27$ . As described in §3.1 there is a rapid decline with increasing redshift in the number of normal galaxies between  $z \approx 1$  and  $z \approx 1.5$ , such that the co-moving density increases by  $8.3 \times 10^3 \text{ Gpc}^{-3} \text{ Gyr}^{-1}$  for ellipticals and  $5.7 \times 10^3 \text{ Gpc}^{-3} \text{ Gyr}^{-1}$  for spirals during this 1.6 Gyr period, roughly a factor of 10 increase in number densities. As discussed briefly in §3.5 this change in morphology is not caused by so-called morphological k-corrections in which galaxies appear different at different wavelengths. It can however be partially produced by selection effects, although a strong drop is also found when considering galaxies at a fixed absolute magnitude (Figure 2). Both spirals and ellipticals with  $M_B < -20$  should be found in the Hubble Deep Fields up to  $z \approx 2$ , and at even higher redshifts if passive evolution is considered (e.g., Conselice et al. 2004b).

The redshift range  $1 < z < 2$  is obviously critical for understanding the final onset and production of the Hubble sequence and the origin of the galaxy structure-redshift relationship. It is also the epoch (during a short 2.5 Gyrs!) where the star formation rate, AGN activity and stellar mass assembly is at its highest. Understanding how the galaxy structure-redshift relationship evolves during this epoch is critical for understanding the causes behind galaxy formation. It is therefore worth spending some time discussing what is found morphologically and structurally in the galaxy population between  $1 < z < 2$ .

Figure 4 shows Advanced Camera for Surveys (ACS) images of the brightest galaxies in the rest-frame optical found within the Chandra Deep Field South Great Observatory Origins Survey (GOODS) imaging. Clearly, there is a rich morphological mix at this redshift, with many galaxies appearing similar to modern ellipticals and spirals, but with important structural differences that make them fundamentally different from modern normal galaxies. Another way to investigate this population is to study systems that have spectral energy distributions that likely place them at  $1 < z < 2$ , such as the extremely red

objects, discussed in §4.1. The images of these galaxies reveal that some are almost normal, with outer shell like features and what appear to be large star forming complexes. Understanding the physical causes behind these features will help reveal the formation mechanisms of galaxies.

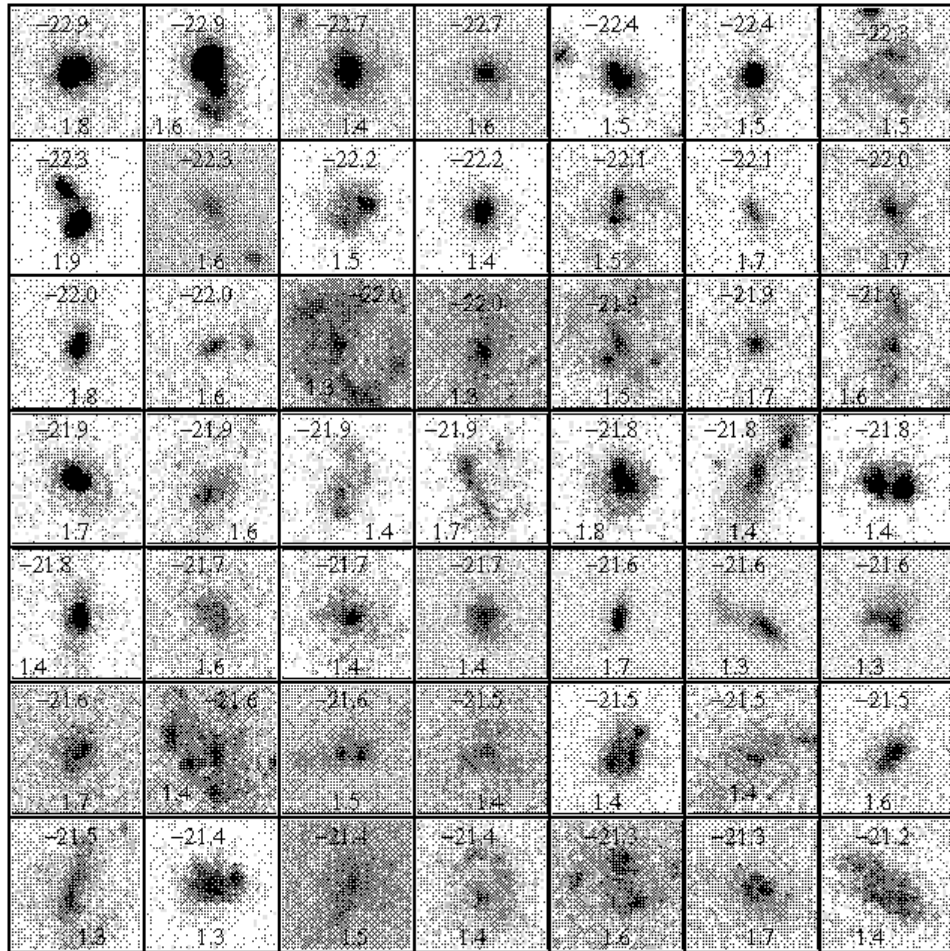


*Figure 4.* The brightest galaxies in ACS GOODS images whose photometric redshifts place them at  $1 < z < 2$ . These are ordered from brightest to faintest down to  $M_B = -21$ . The upper number is the  $M_B$  of each galaxy and the lower number is its redshift. There is a large diversity of properties, from systems that appear very peculiar to those that look similar to normal galaxies. Scale of these images is  $2''$  on each side, corresponding to  $17$  kpc at these redshifts. **See Figure4.gif for a high resolution version.**

### 3.4 Galaxy Structures at High Redshift $z > 2$

The structures and morphologies of galaxies at  $z > 2$  are just now being studied in detail. Early work in this area suggested that galaxies selected by the Lyman-break technique have compact structures with outer light envelopes (Giavalisco et al. 1996). These compact structures have half-light radii a few kpc in size, similar to the bulges of modern spirals or moderate luminosity spheroids. Many of these compact galaxies have steep light profiles and asymmetrically distributed outer nebulosity. The depth of this early imaging was quickly superseded by the Hubble Deep Field North which showed a rich diversity of galaxy structures (Figure 5; Ferguson, Dickinson & Williams 2000). The morphologies of these galaxies is still however a largely unexplored area of parameter space.

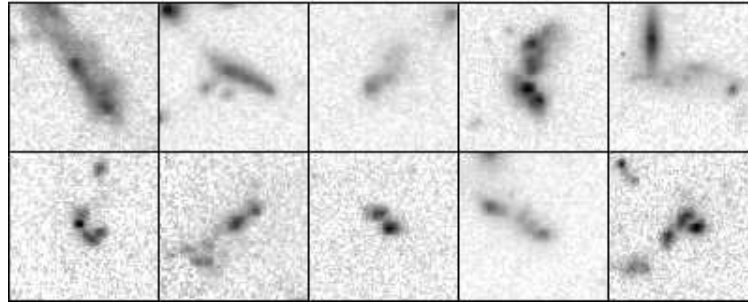


Figure 5. The morphologies of bright galaxies, mostly at  $z > 2$ , in the Hubble Deep Field North showing the peculiar and non-compact structures of these galaxies, many with several bright central regions or knots.

One of the reasons the morphologies of  $z > 2$  galaxies have not been studied in detail is that describing their structures is not a trivial problem, as very few galaxies at high redshift can be identified as objects that would fit on the Hubble Sequence (e.g., Giavalisco et al. 1996; Conselice et al. 2003a; Lotz et al. 2003). One way to approach this problem is to use a purely descriptive approach described above, while another is to use quantitative techniques to characterize these structures. This has been done in Conselice et al. (2003a) and Conselice et al. (2004b) for galaxies at  $z > 2$ . The CAS systems shows that at the highest redshifts there is a real dichotomy in the galaxy population such that the most luminous and most massive galaxies are consistent with undergoing a major merger based on CAS indices, particularly the asymmetry index (Conselice et al. 2003a). What is found is that half of all bright,  $M_B < -21$  or massive  $M > 10^{11} M_\odot$  galaxies are actively undergoing a major merger. The fainter and lower mass galaxies have peak merger fractions at  $z \approx 2.5$  that are only 20%, or lower. The relative fraction of mergers declines at lower

redshifts very quickly for these massive and luminous galaxies as power law  $(1+z)^{-3.5}$  (Conselice et al. 2003). A comparison to hierarchical assembly models of galaxies is shown in Figure 6 using GALFORM simulations (e.g., Benson et al. 2002). These models over-predict the number of major mergers occurring for the brightest galaxies at  $z < 1$ , consistent with the fact that there are too many bright K-band selected galaxies at  $z = 1-1.5$  than predicted in Cold Dark Matter based models (Somerville et al. 2004; see also §4.3).

### 3.5 Morphological K-corrections

A primary problem in understanding the galaxy structure-redshift relationship is constraining the effects of the morphological k-correction, whereby galaxy structure changes as a function of wavelength. The main problem is that most deep high resolution imaging is done in the optical, probing up to  $\lambda = 1 \mu\text{m}$ , allowing for a sampling of the rest-frame optical,  $< 4000 \text{ \AA}$ , only up to  $z = 1.5$ . At redshifts higher than this we begin to sample rest-frame ultraviolet light from galaxies. For galaxies at  $z = 3$ , for example, the z-band filter (F850L) (the reddest GOODS and ACS Hubble Ultra Deep Field filter) samples  $\approx 2500 \text{ \AA}$ , the near ultraviolet, where only young stars with ages  $< 100 \text{ Myrs}$  are sampled.

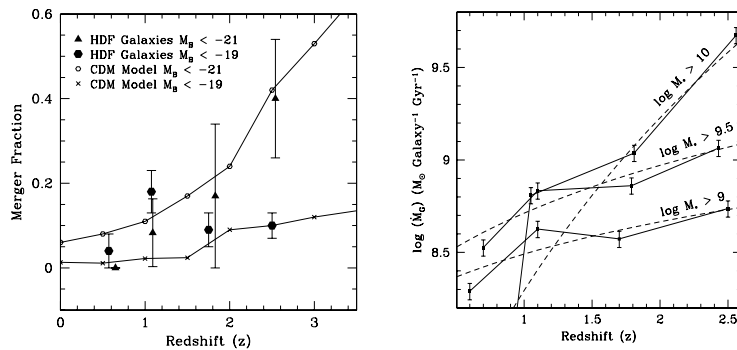


Figure 6. Left panel: major merger fractions to  $z = 3$  at magnitude limits  $M_B = -21$  and  $-19$ . Semi-analytical model predictions are also shown. Right panel: Stellar mass accretion history from major mergers as a function of initial mass (see Conselice et al. 2003a).

This is potentially a problem because both qualitatively, and quantitatively, galaxies have very different structures in their rest-frame optical and UV light (e.g., Bohlin et al. 1991; Kuchinski et al. 2001; Windhorst et al. 2002; Papovich et al. 2003). The largest differences are found for galaxies that are composed of old and young stellar components which are not spatially mixed, such as early type spirals or Hubble classifications Sa and Sb (e.g., Windhorst et al. 2002). The one type of galaxy that looks nearly identical at UV and

optical wavelengths are starbursting galaxies, or galaxies whose structures are dominated by star formation (e.g., Conselice et al. 2000c; Windhorst et al. 2002).

Similarly, when examining galaxies at different redshifts, there are different types of morphological k-corrections, depending on the redshift and galaxy type. At  $z < 1.5$  morphological k-corrections are not an issue as we are able to sample rest-frame optical light from galaxies. At higher redshifts the NICMOS camera on HST allows us to determine the rest-frame optical structures and morphologies, although only limited field coverage exists (e.g., Dickinson et al. 2000). The result of this imaging is that galaxies that look irregular and distorted in the rest-frame UV also appear distorted in the rest-frame optical (Teplitz et al. 1998; Thompson et al. 1999), with some possible and important exceptions (e.g., Giavalisco 2002; Labbe et al. 2003; Conselice et al. 2004a,b). While these are rare systems, they do exist, and examples of morphologically selected ellipticals are found out to  $z > 2$ . These normal galaxies will likely become more common as we probe deeper in the infrared with high resolution wide field imaging.

## 4. The Nature of the Peculiar High- $z$ Galaxy Population

### 4.1 Extremely Red Objects

Extremely red objects (EROs), defined by an optical-infrared color limit, typically using the criteria  $(R-K) > 5-6$ , or  $(I-K) > 4-5$  (e.g., Daddi et al. 2000), were traditionally thought to be early type or dusty galaxies at  $z > 0.8$ . Extremely red galaxies are red because of a large 4000 Å break produced by aged, or dusty, stellar populations. EROs are now also found in the near infrared with a (J-K) limit that locates objects at redshifts  $z > 2$ . The ERO population is therefore a good one for determining the basic properties of evolved galaxies at high redshifts.

The morphologies of EROs are mixed, with a strong redshift dependence (Figure 7). Systems at  $z < 1.2$  are typically early or late-type galaxies, while those at  $z > 1.2$  are more irregular or peculiar (Moustakas et al. 2004). The spectra of EROs are also mixed, with about half showing signs of evolved stellar populations, with the other half showing emission lines (Cimatti et al. 2002). Morphological studies of EROs demonstrate that a large fraction, perhaps the majority of the  $K < 20$  objects, are disks (Yan & Thompson 2003). It thus appears likely that the ERO definition, far from finding only specific galaxy populations, is sampling all morphological types. This is a good sample for studying galaxies evolving onto the Hubble sequence since Hubble types are the most evolved galaxies at  $z = 0$  and are likely also the most evolved at  $z = 1$ . This has been done by e.g., Moustakas et al. (2003) who studied the redshift distributions of EROs in the GOODS-South field as a function of mor-

phology. Moustakas et al. found that the lower redshift EROs are dominated by regular galaxies, while higher redshift samples at  $z > 1.5$  are dominated by galaxies that cannot be placed on the Hubble sequence (Figure 7).

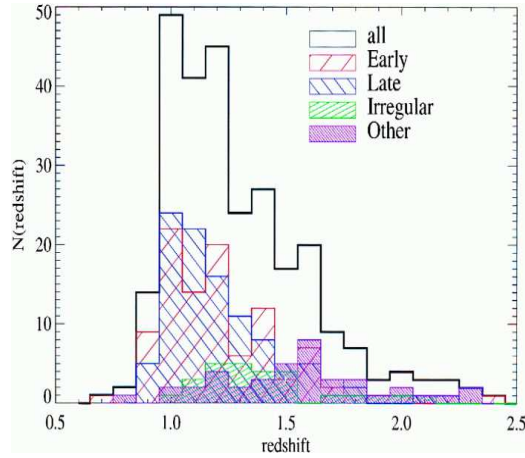


*Figure 7.* The redshift distributions for extremely red galaxies from the GOODS-South field (Moustakas et al. 2004) showing how the morphological distribution for this population shifts to the 'other' or peculiar types at higher redshifts.

Recently, there have been claims of a new population of red galaxies at  $z > 2$ . These are similar to the lower redshift ERO population in that they are identified by a color cut that isolates galaxies based on the Balmer break, but uses the color defined by two infrared filters, normally the J and K bands (e.g.,  $(J-K) > 2.3$ ). These systems are typically at  $z > 2$  and may be quite distinct from the Lyman-break galaxy population (Franx et al. 2003; van Dokkum et al. 2004). The morphologies of these systems have not been studied in detail, partially because there are so few examples, yet bright K-band selected galaxies at  $z > 2$  and with  $K < 20$  often have irregular UV morphologies (Labbe et al. 2003; Daddi et al. 2004) indicating star formation. There are however some hints for spiral structures and more regular compact near infrared morphologies in some of these systems (Labbe et al. 2003; Daddi et al. 2004). These infrared EROs have large stellar masses and are generally consistent, based on clustering analyses and stellar population arguments, with the most evolved systems at high redshift. These galaxies are therefore the best candidates for being the progenitors of evolved galaxies found in dense regions today.

## 4.2 Luminous Diffuse Objects and Chain Galaxies

In Conselice et al. (2004) a new galaxy type, found abundantly between  $1 < z < 2$ , is described and characterized. These galaxies, which have no local counterparts, were discovered based on their low light concentrations and high luminosities, and are called Luminous Diffuse Objects (LDOs). These objects are fairly common with surface densities  $1.8 \text{ arcmin}^{-2}$ , and co-moving number densities of  $5 \times 10^5 \text{ Gpc}^{-3}$  within the GOODS South field (Conselice et al. 2004). These objects were independently discovered by Elmegreen et al. (2004a) and are likely face on counterparts of the ‘chain galaxies’ discussed in Cowie et al. (1995) (Elmegreen et al. 2004b).

Elmegreen et al. (2004b) compared the colors of the star forming knots in their sample of LDOs with the knots found in chain galaxies, finding a very similar color distribution. This suggests that chain galaxies are the edge-on versions of LDOs. Both chain galaxies and LDOs are known to be large complexes of star forming regions (Cowie et al. 1995; Conselice et al. 2004a). Formation scenarios for these systems are discussed in Elmegreen et al. (2004b), and are consistent with large amounts of star formation occurring after gas in an initial disk fragments and produce several large clumps. In models, these clumps are predicted to form through energy dissipation and later merge together to form bulges (Immeli et al. 2004). The fact that there are no obvious bulge components in LDOs is a clue that bulge formation may occur *after* disk formation, not before, as is generally assumed in hierarchical models.

LDOs are likely in a phase where a large fraction of their stellar mass is being assembled. The star formation rate in LDOs is on average  $4 \text{ M}_{\odot} \text{ year}^{-1}$  before correcting for dust, and they have starburst spectral energy distributions (Figure 8). These systems account for up to 50% of all the star formation occurring between  $1 < z < 2$ , where a large fraction of the stellar mass in galaxies formed (Dickinson et al. 2003). The effective radii of these galaxies varies from 1.5 - 10 kpc, and for these and other reasons a fraction of them are likely disks in formation (Conselice et al. 2004; Elmegreen et al. 2004b; Figure 8).

## 4.3 Galaxy Mergers

A major, but still largely under-studied, aspect of galaxy formation is the role of galaxy mergers. The merging of galaxies to form larger systems is the cornerstone of the idea behind the modern galaxy formation model, dark matter, and cosmology (e.g., Cole et al. 2000). Constraining this process observationally is just now being done. The first problem is identifying, confidently, which galaxies at high redshift are undergoing a major merger (defined as a merger mass ratio 3:1 or lower). There are a few methods for finding galaxies which are merging, or which soon will. The traditional method for identifying

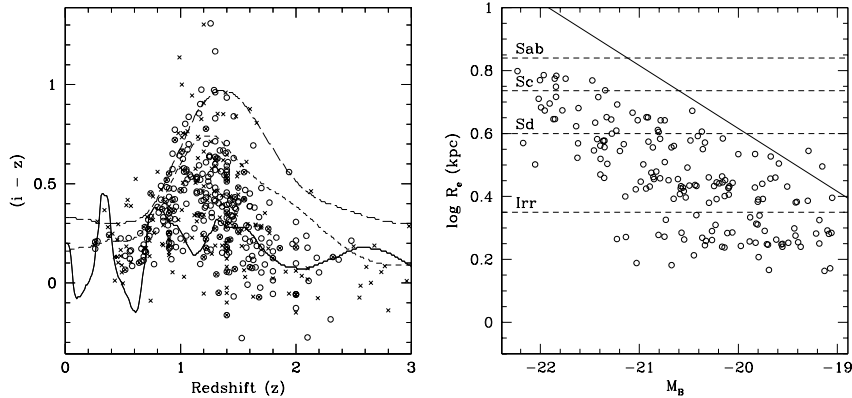


*Figure 8.* Left panel: The distribution of  $(i - z)$  colors for LDOs (circles) as a function of redshift with two Coleman, Wu and Weedman spectral energy distributions and a Kinney et al. starburst model plotted (see Conselice et al. 2004a). These are from bluest to reddest - starburst (solid line), Scd (dashed), Sbc (long dashed). Right panel: Absolute magnitude-effective radius relationship for LDOs. The solid line is the canonical Freeman disk relationship at  $z = 0$ . The dashed horizontal lines show the effective radii of different nearby galaxy types.

mergers is to identify galaxies in kinematic pairs that are close ( $< 20$  kpc), and at nearly the same radial velocity (with  $< 500$  km s $^{-1}$ ). Identifying pairs at high redshift in this manner is difficult due to the inability to determine radial velocities for complete samples, and it is thus largely applicable only at redshifts  $z < 1$ .

A promising method explored in Conselice (2003) is identifying galaxy mergers which are in progress, that is systems that have already merged and are undergoing dynamical relaxation. One way to identify these systems is through their chaotic kinematic structures revealed through integral field spectroscopy or velocity curves (e.g., Erb et al. 2004). Alternatively, and more commonly, is to use the stellar structures of galaxies. In §2 the methods and reasoning behind using the asymmetry index to find mergers are explained, and the results of these techniques applied to high redshift galaxies are described in §3.4.

Since the modern paradigm for forming galaxies implicitly assumes massive galaxies form by merging, it is important to test this idea. The agreement between Cold Dark Matter based models and the data, shown in Figure 6, is good at high redshift, but fails by a significant amount to reproduce the merger fractions for bright galaxies at lower redshifts. This is likely because massive galaxies are forming earlier than low mass galaxies, which may or may not be an effect of environment - massive galaxies are also more likely to be found in dense areas (Dressler 1980). We examine this in more detail to determine how the stellar masses of high redshift galaxies are built up through mergers

and the star formation induced by this merging. The amount of stellar mass added to a galaxy during an observed major merger, assuming a mass ratio of 1:1, can be calculated from the star forming properties of galaxies and the mass accretion rate from merging (e.g., Papovich et al. 2001; Figure 6). Based on the merger rates calculated in Conselice et al. (2003a), a typical Lyman-break galaxy at  $z \approx 3$  will undergo  $\approx 5$  major mergers, with accompanying star formation, before  $z \approx 1$  and is unlikely to have a major merger at  $z < 1$ . The mass added by each of these mergers, plus the likely amount of new stars produced in star formation, is enough to create a  $> M_{\odot}$  (Cole et al. 2001) galaxy by  $z = 1$ . This also suggests that the galaxy structure-redshift relationship can be described as a cooling of the galaxy population from an era of rapid mergers that has been steadily declining since  $z \approx 3$ .

Minor mergers are harder to constrain, yet are likely a major method for adding material to normal galaxies at  $z < 1$  (e.g., Patton et al. 2002; Bundy et al. 2004). This method, or secular evolution, are the most likely possibilities for driving evolution in the galaxy population at  $z < 1$ , when up to 50% of all stellar mass formed.

#### 4.4 High Redshift Luminous Infrared Galaxies

A significant galaxy population at high redshift is the luminous infrared galaxies detected by redshifted mid-infrared emission from dust grains at observed wavelengths 10 - 1000  $\mu\text{m}$ . The existence of these sources is suggested by the large far-IR and sub-millimeter backgrounds (Puget et al. 1996). These luminous infrared sources are very common at  $z > 2$ , over an order of magnitude as common as their local counterparts (Chapman et al. 2003a). With the launch of the *Spitzer Space Telescope* the study of these galaxies is very much in progress, although important features of these galaxies are already known. Luminous infrared galaxies in the nearby universe are found to be heated by a mixture of AGN activity and star formation (Sanders & Mirabel 1996), although the most luminous sources with  $L > 10^{12} L_{\odot}$  are nearly all starburst-induced major mergers. The relative contributions at high redshift is also a mixture of these two types, although preliminary *Spitzer* observations show that the spectral energy distributions of high redshift luminous infrared galaxies are largely composed of star forming systems (Frayser et al. 2004).

The rest-frame UV (or observed optical) properties of sub-mm sources observed with the Hubble Space Telescope reveal that these galaxies would be included in magnitude limited optical studies (such as the HDF) and that their structures are very peculiar in appearance (e.g., Chapman et al. 2003b). There are two pieces of evidence that suggests these morphologically peculiar sub-mm/radio selected luminous infrared galaxies at  $z > 2$  are undergoing major galaxy mergers. The first is the very large line widths found in CO mapping

(Genzel et al. 2004). Galaxies with similar large velocity widths in the nearby universe are undergoing major mergers (Conselice et al. 2000b). The other evidence is that the morphologies of sub-mm sources are generally peculiar (e.g., Chapman et al. 2003b) and are quantitatively consistent with undergoing major mergers (Conselice et al. 2003b). The merger fraction for sub-mm detected galaxies is in fact higher than for the most massive Lyman-break galaxies (Conselice et al. 2003b). This suggests that the most massive galaxies at high redshift, which are probably these sub-mm sources (Tecza et al. 2004), are forming by mergers.

## 5. Relationship to the Dark Universe

The structures of galaxies, and the evolution of structures, potentially relates directly with the existence of dark matter, dark energy and black holes. I only briefly discuss this here as much of this is work for the future. One example is that galaxy mergers might not occur as commonly without the dynamical friction produced by dark matter halos (e.g., Sellwood 2004). Detailed modeling of this however has not yet been done. As discussed, black holes are directly traceable with the concentration of galaxy light ( $\kappa^2$ ). Dark energy is also likely imprinting its effects, and is perhaps the fundamental cause of the morphology-redshift relationship.

The relationship between the velocity dispersion of spheroids and the mass of their central black holes (Gebhardt et al. 2000; Ferrarese & Merritt 2000) is a fundamental property of spheroids. This relationship, which is effectively between the scale of a spheroid system and its central black hole, is also projected in the concentration index-black hole mass relationship. This relationship appears to hold to some degree up to  $z \approx 1.2$  based on the correlation between galaxies with X-ray emission and the CAS concentration index (Grogin et al. 2003). X-ray sources up to  $z \approx 1.2$  are found in galaxies with the highest light concentrations, suggesting that the bulge/central black hole relationship is in place by these redshifts. Understanding this relationship at higher redshift, as well as how dark matter condenses and evolves with galaxy structure, are topics for future investigations with 20-30 meter ground based telescopes and the James Webb Space Telescope.

## 6. Acknowledgments

It is a pleasure to acknowledge my collaborators and colleagues, especially Mark Dickinson, Richard Ellis, Kevin Bundy, and Casey Papovich for helping shape my evolving understanding of this material. Thanks also to Colin Borys and Kevin Bundy for comments on this manuscript. I also thank David Block and the organizing committees for inviting me to present this contribution and their patience in receiving this review.

**References**

- Abraham, R.G., et al. 1996, *ApJS*, 107, 1  
Andersen, D.R., et al. 2001, *ApJ*, 551, 131L  
Bell, E.F., et al. 2004, *ApJ*, 608, 752  
Benson, A.J., Lacey, C.G., Baugh, C.M., Cole, S., & Frenk, C. 2002, *MNRAS*, 333, 156  
Bershady, M.A., Jangren, A., & Conselice, C.J. 2000, *AJ*, 119, 2645  
Binggeli, B., & Cameron, L.M. 1991, *A&A*, 252, 27  
Blumenthal, G.R., et al. 1984, *Nature*, 311, 517  
Brinchmann, J., & Ellis, R.S. 2000, *ApJ*, 536, 77L  
Bundy, K., Fukugita, R.S., Ellis, R.S., Kodama, T., & Conselice, C.J. 2004, *ApJ*, 600, 123L  
Caon, N., Capaccioli, M., & D'Onofrio, M. 1993, *MNRAS*, 265, 1013  
Chapman, S.C., Blain, A.W., Ivison, R.J., & Smail, I.R. 2003, *Nature*, 422, 695  
Chapman, S.C., Windhorst, R., Odewahn, S., Yah, H., Conselice, C. 2003b, *ApJ*, 599, 92  
Cimatti, A., et al. 2002, *A&A*, 381, L68  
Cole, S., Lacey, C.G., Baugh, C.M., & Frenk, C.S. 2000, *MNRAS*, 319, 168  
Cole, S., et al. 2001, *MNRAS*, 326, 255  
Conselice, C.J., Bershady, M.A., & Jangren, A. 2000a, *ApJ*, 529, 886  
Conselice, C.J., Bershady, M.A., & Gallagher, J.S. 2000b, *A&A*, 354, 21L  
Conselice, C.J., et al. 2000c, *AJ*, 119, 79  
Conselice, C.J. 2003, *ApJS*, 147, 1  
Conselice, C.J., Bershady, M.A., Dickinson, M., & Papovich, C. 2003a, *AJ*, 126, 1183  
Conselice, C.J., Chapman, S.C., Windhorst, R.A. 2003b, *ApJ*, 596, 5L  
Conselice, C.J., et al. 2004a, *ApJ*, 600, L139  
Conselice, C.J., Blackburne, J., & Papovich, C. 2004b, *astro-ph/0405001*  
Cowie, L.L., Hu, E.M., & Songaila, A. 1995, *AJ*, 110, 1576  
Daddi, E., et al. 2004, *ApJ*, 600, 127L  
Daddi, E., Cimatti, A., & Renzini, A. 2000, *A&A*, 362, 45L  
de Vaucouleurs, G., et al. 1991, "Third Reference Catalogue of Bright Galaxies"  
Dickinson, M., Papovich, C., Ferguson, H.C., & Budavari, T. 2003, *ApJ*, 587, 25  
Dickinson, M., et al. 2000, *ApJ*, 531, 624  
Dressler, A. 1980, *ApJ*, 236, 351  
Driver, S.P., Windhorst, R.A., & Griffiths, R. 1995, *ApJ*, 453, 48  
Elmegreen, B.G. 2002, *ApJ*, 577, 206  
Elmegreen, D.M., Elmegreen, B.G., & Hirst, A.C. 2004a, *ApJ*, 604, 21L  
Elmegreen, D.M., Elmegreen, B.G., & Sheets, C.M. 2004b, *ApJ*, 603, 74  
Erb, D.K., Steidel, C.C., Shapley, A.E., Pettini, M., & Adelberger, K.L. 2004, *astro-ph/0404235*  
Ferguson, H.C., Dickinson, M., & Williams, R. 2000, *ARA&A*, 38, 667  
Ferguson, H.C., et al. 2004, *ApJ*, 600, 107L  
Ferrarese, L., & Merritt, D. 2000, *ApJ*, 539, 9L  
Franx, M. et al. 2003, *ApJ*, 587, 79L  
Frayser, D.T., et al. 2004, *astro-ph/0406351*  
Fukugita, M., Hogan, C.J., & Peebles, P.J.E. 1998, *ApJ*, 503, 518  
Gebhardt, K., et al. 2000, *ApJ*, 539, 13L  
Genzel, R., et al. 2004, *astro-ph/0403183*  
Giavalisco, M., Steidel, C., Macchetto, F.D. 1996, *ApJ*, 470, 189  
Giavalisco, M. 2002, *ARA&A*, 40, 579  
Giavalisco, M. et al. 2004, *ApJ*, 600, L93  
Glazebrook, K., et al. 2004, *astro-ph/0401037*  
Glazebrook, K., et al. 1995, *MNRAS*, 275, 19L

- Graham, A., Lauer, T.R., Colless, M., & Postman, M. 1996, ApJ, 465, 534  
Graham, A., Erwin, P., Caon, N., & Trujillo, I. 2001, ApJ, 563, 11L  
Grogin, N., et al. 2003, ApJ, 595, 684  
Immeli, A., Samland, M., Westera, P., & Gerhard, O. 2004, astro-ph/0406135  
Kajisawa, M., & Yamada, T. 2001, PASJ, 53, 833  
Kuchinski, L.E., Madore, B.F., Freedman, W.L., & Trewhella, M. 2001, AJ, 122, 729  
Larson, R.B. 1975, MNRAS, 173, 671L  
Labbe, I., et al. 2003, ApJ, 591, 95L  
Lotz, J.M., Primack, J., & Madau, P. 2003, astro-ph/0311352  
Marzke, R.O., et al. 1998, ApJ, 503, 617  
Madau, P., et al. 1996, MNRAS, 283, 1388  
Mobasher, B., et al. 2004, ApJ, 600, 143L  
Moustakas, L.A., et al. 2004, ApJ, 600, 131L  
Papovich, C., et al. 2003, ApJ, 598, 827  
Papovich, C., Dickinson, M., & Ferguson, H.C. 2001, ApJ, 559, 620  
Patton, D.R., et al. 2002, ApJ, 565, 208  
Peng, C.Y., Ho, L.C., Impey, C.D., & Rix, H.-W. 2002, AJ, 124, 266  
Puget, J.-L., et al. 1996, A&A, 308, 5  
Rix, H.-W., et al. 2004, ApJS, 152, 163  
Roberts, M.S., & Haynes, M.P. 1994, ARA&A, 32, 115  
Sanders, D.B., & Mirabel, I.F. 1996, ARA&A, 34, 749  
Schombert, J.M. 1986, ApJS, 60, 603  
Sellwood, J.A. 2004, astro-ph/0401398  
Somerville, R.S., Primack, J.R., & Faber, S.M. 2001, MNRAS, 320, 504  
Somerville, R.S., et al. 2004, ApJ, 600, 135L  
Stanford, A., et al. 2004, AJ, 127, 131  
Takamiya, M. 1999, ApJS, 122, 109  
Tecza, M., et al. 2004, ApJ, 605, 109L  
Teplitz, H., Gardner, J., Malmuth, E., & Heap, S. 1998, ApJL, 507, 17L  
Thompson, R.I., et al. 1999, AJ, 117, 17  
Tinsley, B.M., & Gunn, J.E. 1976, ApJ, 203, 52  
van den Bergh, S., Cohen, J., Crabbe, C. 2001, AJ, 122, 611  
van Dokkum, P. et al. 2004, astro-ph/0404471  
White, S.D.M., & Rees, M.J. 1978, MNRAS, 183, 341  
White, S.D.M., & Frenk, C.S. 1991, ApJ, 379, 52  
Windhorst, R.A., et al. 2002, ApJS, 143, 113  
Yan, L., & Thompson, D. 2003, ApJ, 586, 765

This figure "Figure4.gif" is available in "gif" format from:

<http://arxiv.org/ps/astro-ph/0407463v1>